Cyclic porphyrin arrays as artificial photosynthetic antenna: synthesis and excitation energy transfer

Yasuyuki Nakamura, Naoki Aratani and Atsuhiro Osuka*

Received 27th February 2007
First published as an Advance Article on the web 29th March 2007
DOI: 10.1039/b618854k

Covalently linked cyclic porphyrin arrays have been explored in recent years as artificial photosynthetic antenna. In this review we present the fundamental aspects of covalently linked cyclic porphyrin arrays by highlighting recent progress. The major emphasis of this *tutorial review* lies on the synthetic method, the structure, and the excitation energy transfer (EET) of such arrays. The final cyclization steps were often performed with the aid of templates. Efficient EET along the wheel is observed in these cyclic arrays, but ultrafast EET processes with rates of <1 ps, which rival those in the natural LH2, are rare and have been identified only in cyclic arrays **30–32** composed of directly *meso–meso* linked porphyrins.

1 Introduction

Nature is often the ultimate goal for chemists. Photosynthesis is one of the most important natural processes. During photosynthesis, plants convert light energy into electrochemical energy and eventually into chemical potential energy stored in carbohydrates and other compounds. The carbohydrates are oxidized to provide energy to the living organism. The importance of photosynthesis has driven many researchers to look for ways to duplicate the fundamental features of photosynthesis in simplified systems. Photosynthesis starts by the absorption of a photon by light-harvesting (antenna) complexes that usually comprise a large number of pigments embedded in protein matrices. This process is followed by an efficient energy migration over many pigments within the antenna system until a reaction center is encountered.

In 1995, the crystal structure of the light-harvesting antenna complex LH2 of the purple bacterium *Rhodopseudomonas acidophila* was elucidated to be circularly arranged chromophoric assemblies (Fig. 1).[1–3] Since the advent of this wheel-like structure, many efforts were made towards the synthesis of cyclic porphyrin arrays to study excitation energy transfer (EET) along the cyclic arrays. Although the primary motivation for the synthesis of cyclic porphyrin arrays is to duplicate the structure and function of the natural light-harvesting antennae, large and shape-persistent structures of such porphyrin wheels have evoked different interest in the fields of host–guest chemistry, single molecule photochemistry, and so on. There are many reviews on the topic of molecular-level artificial photosynthesis.[4–8] In this review, we focus on the

Department of Chemistry, Graduate School of Science, Kyoto University, and Core Research for Evolutional Science and Technology (CREST), Japan Science and Technology Agency, Sakyo-ku, Kyoto 606-8502, Japan. E-mail: osuka@kuchem.kyoto-u.ac.jp; Fax: +81 75 743 3970

Yasuyuki Nakamura

Yasuyuki Nakamura was born in 1980 in Ohta, Japan. He received his BSc (2003) and MSc (2005) degrees from Kyoto University. He is currently a PhD student with Professor A. Osuka at the same university, focusing on the synthesis and exploration of directly linked porphyrin arrays. During autumn of 2006, as a visiting fellow, he worked with Professor Michael R. Wasielewski's group at Northwestern University. He was selected as a Research Fellow of the Japan Society for the Promotion of Science (JSPS) in 2005.

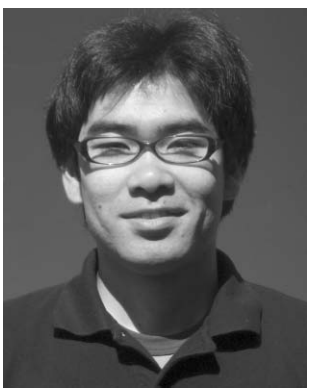

Naoki Aratani

Naoki Aratani was born in 1975 in Nagoya, Japan. He received his BSc (1999) and MSc. (2001) degrees from Kyoto University. He was selected as a Research Fellow of the Japan Society for the Promotion of Science (JSPS) in 2001. He received his PhD degree from Kyoto University in 2005 on the chemistry of meso–meso linked porphyrin arrays. In 2003, he started an academic career at the Department of Chemistry of Kyoto University as an assistant professor with Prof. A. Osuka, focusing on the design and synthesis of extremely long porphyrin arrays for the exploration of the nature of giant molecules. In 2006, he joined Professor Omar M. Yaghi's group as a visiting scientist at the University of California, Los Angeles, studying porous crystalline materials.

This journal is © The Royal Society of Chemistry 2007

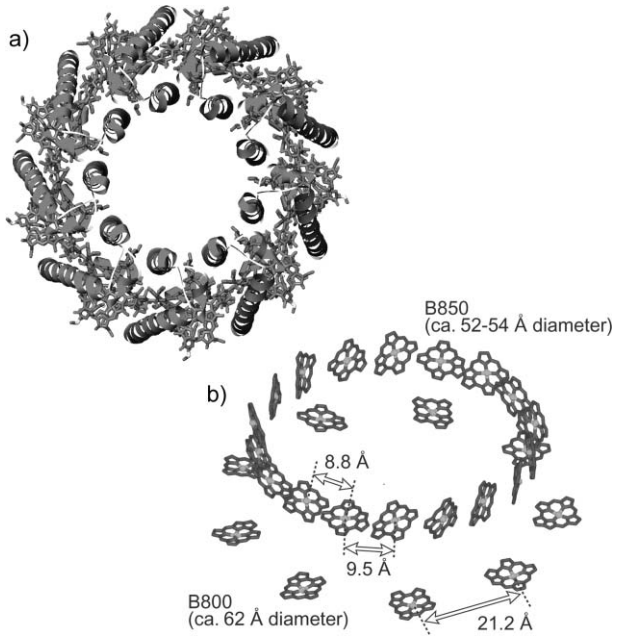

Fig. 1 Crystal structure of LH2 complex. (a) Schematic representation of the overall structure, and (b) structure of B800 and B850 rings. Only skeletons of the macrocycles are shown in (b).

recent developments of cyclic porphyrin arrays, with particular attention to synthetic methods and EET processes.

Cyclic porphyrin arrays are constructed either by means of covalent bonds, noncovalent bonds, or metal coordination bonds.[9–16] Covalently bonded arrays are structurally the most robust but are often difficult to make. The final macrocyclization steps are the most tedious and need the assistance of a template, which helps a precursor to take a favorably folded conformation for cyclization. Noncovalently assembled arrays are usually affected by the environment such as the solvent. Coordination bound porphyrin arrays often use nitrogen atom–metal coordination bonds, *e.g.* pyridine to a zinc atom of a metalloporphyrin or transition metals such as Re, Ru, Pd, and Pt.[11–16] An advantage of these coordinatively bonded arrays is their relatively easy synthetic accessibility, in that appropriately designed components are almost automatically self-assembled to form large arrays. This assembling process is especially effective for the construction of a discrete cyclic array owing to the associated entropic advantage. However, it is to be noted that such coordinatively bonded arrays are sensitive to their environment. For instance, dissociation of the array occurs in coordinating solvents or in the presence of competing coordinating species.

LH2 complex is an $\alpha_a\beta_a$ circular nonamer including two wheel-like assemblies of bacteriochlorophyll (BChl) *a* molecules named as B800 and B850 for their absorption maximum wavelengths (Fig. 1). B800 and B850 rings contain 9 and 18 BChl *a* molecules, that is, one and two per αβ-apoprotein pair, respectively. The wheel diameter of B800 is *ca.* 62 Å, and that of B850 is *ca.* 52–54 Å. In B800, the interchromophore distance is uniform with a Mg–Mg distance of 21.2 Å, and BChl *a* molecules may be regarded as monomeric in nature, since the electronic interaction between BChl *a* molecules is small. In B850, however, each BChl *a* molecule forms a slipped-cofacial dimeric subunit with a Mg–Mg distances of 8.8 Å within an αβ pair, and 9.5 Å from one αβ pair to the next. The crystal structure of LH1 has been revealed to possess a BChl *a* wheel composed of 15 pairs of dimeric subunits (total 30 BChl *a* molecules).[3] This gigantic structure may encourage further synthetic efforts towards even larger cyclic porphyrin arrays.

2 Synthesis of cyclic porphyrin arrays

Template-directed synthesis by Sanders *et al.* provided shape persistent cyclic porphyrin arrays behaving as nanosize enzyme-like functional hosts.[17–20] The versatile but quite effective potential of the template-directed method was demonstrated by the synthesis of a series of cyclic porphyrin oligomers **2**, **3** and **4** with diphenylbutadiyne bridges (Scheme 1). Without a template, the Glaser–Hay coupling reaction of monomer **1** at 5×10^{-4} M concentration gave cyclic products **2** and **3** in 20–25 and 30–35% yields, respectively. In the presence of an appropriate template, the yield of the target compound was increased and the formation of unwanted porphyrin oligomers was largely suppressed. The yield of **2** was increased to 72% with bidentate template **5**, while the use of tridentate template **6** resulted in 52% yield of **3**, hence demonstrating the shape of a template can dictate preferred cyclic porphyrin products. As a more remarkable example, the cyclic tetramer **4** was synthesized from a linear tetramer with tetrakis(4-pyridyl) porphyrin template **7** in an excellent yield (>90%) (Scheme 2).

Lindsey *et al.* reported the syntheses of square porphyrin tetramer **8** and cyclic porphyrin hexamer **11** having diphenylethynyl bridges.[21–24] Square tetramer **8** was synthesized by one-step Sonogashira coupling reaction of **9** and **10** (Scheme 3). To prevent the insertion of copper ion into the free base porphyrins, this Sonogashira coupling was performed under copper-free conditions which they had developed previously

Atsuhiro Osuka

Atsuhiro Osuka was born in 1954 in Gamagori, Japan. He received his PhD degree from Kyoto University in 1982 on the photochemistry of epoxyquinones. In 1979, he started an academic career at the Department of Chemistry of Ehime University as an assistant professor. In 1984, he moved to the Department of Chemistry of Kyoto University, where he became a professor of chemistry in 1996. He was awarded the CSJS Award for Young Chemists in 1988 and the Japanese Photochemistry Association Award in 1999. His research interests cover many aspects of synthetic approaches toward the artificial photosynthesis and development of porphyrin-related compounds with novel structures and functions. He was selected as a project leader of Core Research for Evolutional Science and Technology (CREST) of JST.

This journal is © The Royal Society of Chemistry 2007

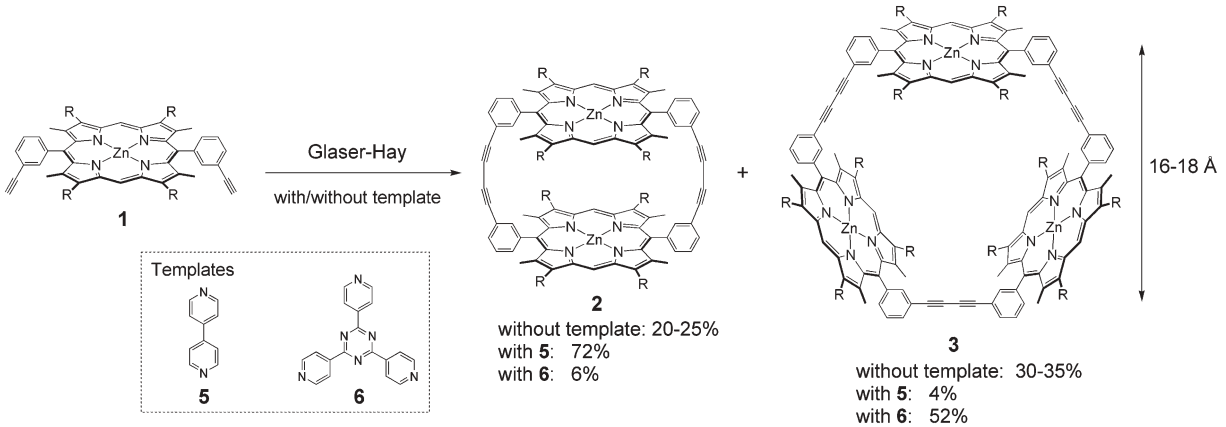

Scheme 1 Reaction conditions: CuCl, TMEDA, CH_2Cl_2, air (R = $CH_2CH_2CO_2CH_3$).

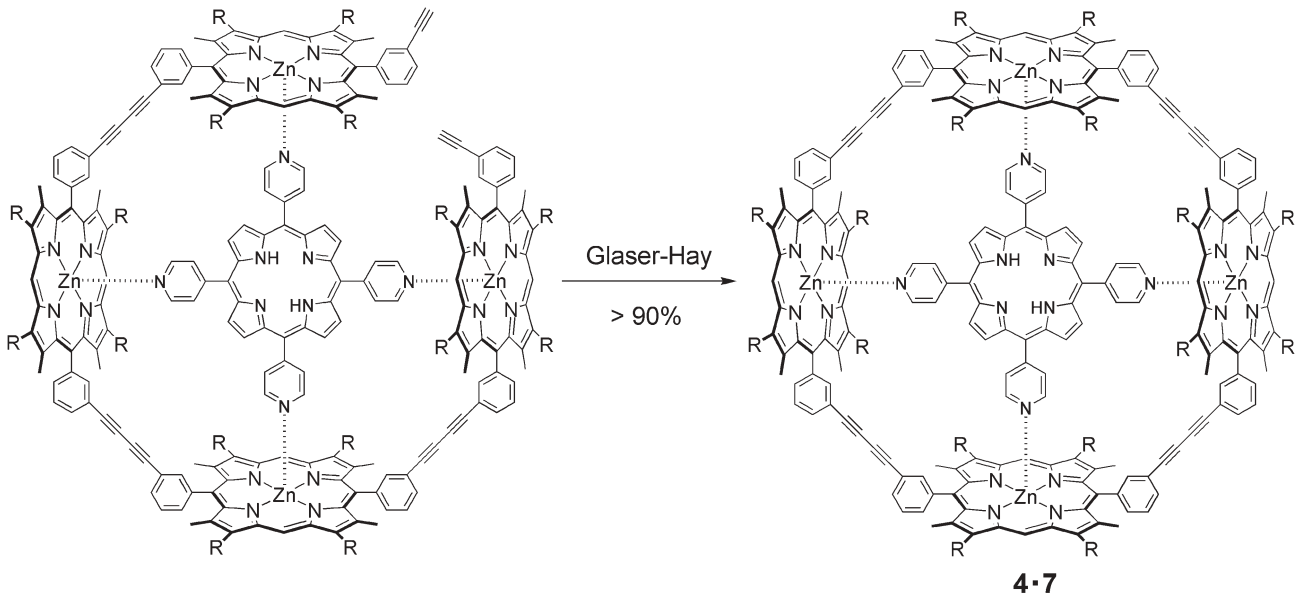

Scheme 2 Reaction conditions: CuCl, TMEDA, CH_2Cl_2, air (R = $CH_2CH_2CO_2CH_3$).

for the synthesis of free base and zinc porphyrin dimers having the same bridge.[25] Use of $AsPh_3$ instead of PPh_3 which has been used for other palladium catalyzed reactions increased the coupling yield to 7% at substrate concentrations of 2.5×10^{-3} M.

Cyclic hexamer **11a** was synthesized by one-step template-directed Sonogashira reaction, in which **12a** and **13b** were coupled under similar conditions in the presence of tridentate guest molecule **14** (Scheme 4). Very detailed studies led to the molecular design of the template **14**. The optimized yield 5.3–5.5% was attained at substrate concentrations of 2.5×10^{-3} M, which were the same conditions used for the synthesis of **8**. A template effect for the synthesis of **11a** was obvious, in that one-step synthesis of **11a** from the monomer components

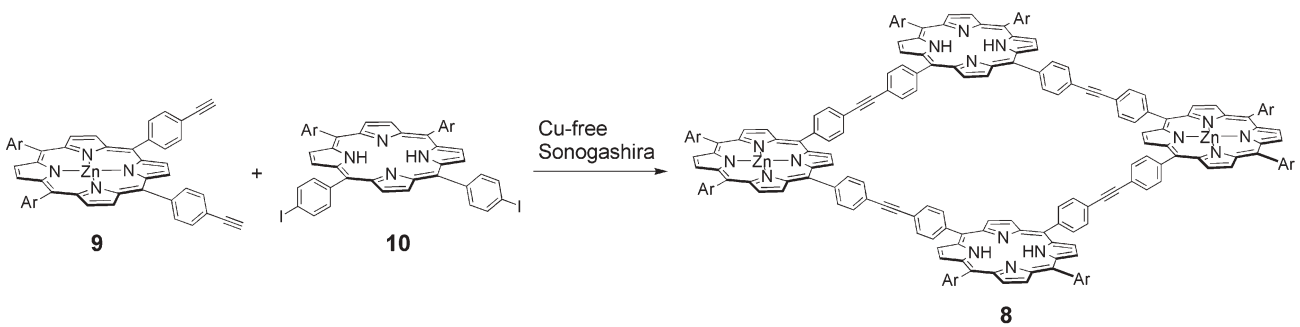

Scheme 3 Reaction conditions: $Pd_2(dba)_3$, $AsPh_3$, toluene, triethylamine (Ar = mesityl).

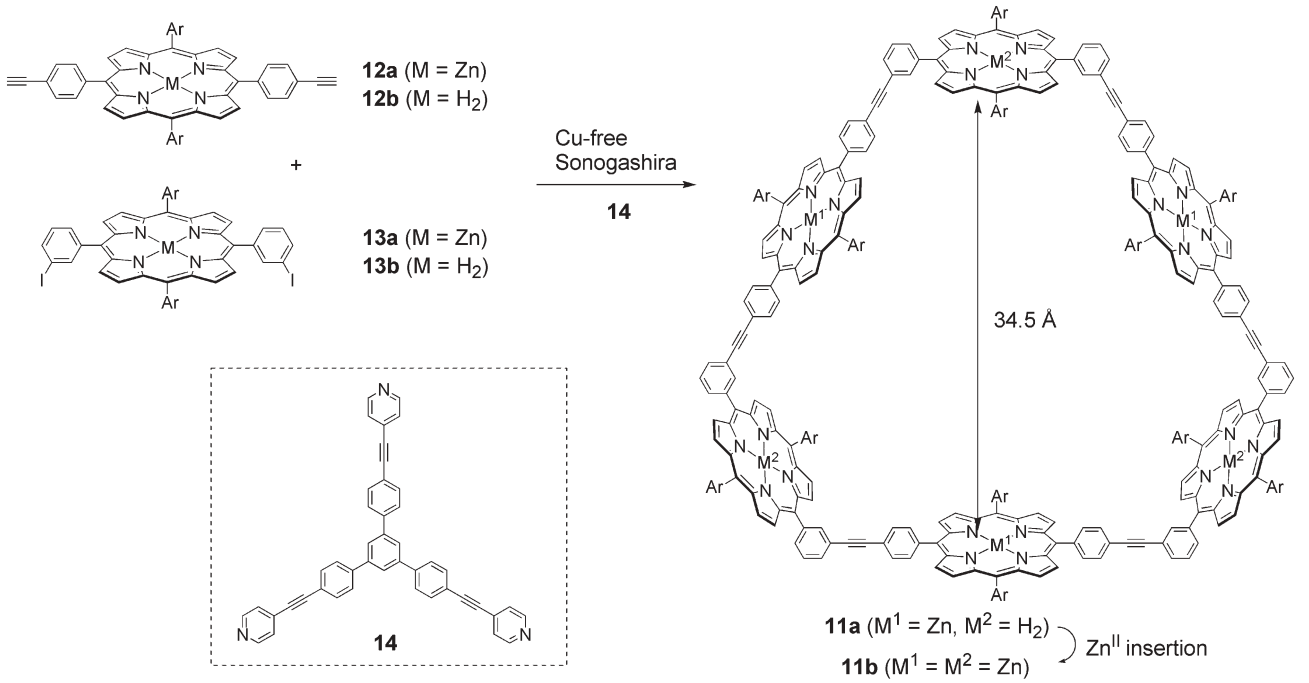

Scheme 4 Reaction conditions: $Pd_2(dba)_3$, $AsPh_3$, toluene, triethylamine (Ar = mesityl).

12a and **13b** without a template molecule gave merely a complicated mixture of oligomers. The importance of the structural complementarity between the substrates and template was well demonstrated by the similar reaction of **12b** and **13a** which failed to produce the corresponding cyclic hexamer. A similar hexamer was also synthesized by a stepwise oligomerization–cyclization sequence with the final 5 + 1 or 3 + 3 cyclization in 10–13% yields using the same template.[23]

Gossauer *et al.* reported cyclic hexamers **15a–c** having 1,3-bis(phenylethynyl)phenylene bridges (Scheme 5).[26–28] They employed the synthetic strategy used for the synthesis of oligophenyleneacetylenes.[29–31] Selective activation of the terminal functional groups enables the step-by-step synthesis of large arrays. The TMS protecting group can be deprotected with aqueous NaOH solution, while the diethyltriazene group can be iodinated with methyl iodide, and these conversion reactions do not affect each other. This procedure is outlined as follows: the compound **A** having both TMS-ethynyl and triethyltriazene groups can be transformed to compounds **B** and **C**, which have ethynyl and iodo groups as reactive sites, respectively. Then, **B** and **C** are coupled to afford compound **A′** that is a larger analogue of **A** (Scheme 6). This method makes it possible to synthesize porphyrin arrays with various different metallation states. Multistep synthesis of the porphyrin array was completed by the final cyclization of linear porphyrin hexamers **16a–c**. High dilution conditions were favorable for cyclization to prevent the intermolecular reaction. Without a template, the yield of cyclic hexamer was 8–31%, differing in metallation state, at the substrate concentration of 2.5×10^{-4} M, but the reproducibility was low for reasons that were unclear.

The cyclization yield was significantly improved with the aid of templates (Fig. 2).[28] In the presence of tridentate template **19** which was designed to fit into the cavity of the macrocycle **15**, the cyclization yield from linear hexamer **16c** was improved to 59% with high reproducibility. Besides the best-fitting template **19**, smaller and larger templates **20** and **21** were also examined for the macrocyclization, which showed crucial effects of the template size for yields of cyclic products. Use of large template **21** led to formation of the hexamer **15c** from **16c** in 45% yield along with polymeric products. In contrast, the cyclization with small template **20** did not provide the hexameric porphyrin ring. As a more advantageous route, the coupling reaction of porphyrin monomer components **17** and **18** at 5.3×10^{-4} M gave the cyclic hexamer **15c** in modest yield (~7%) in the presence of the template **19**.

Sugiura *et al.* reported conjugated square porphyrin tetramer **22** and dodecamer **24** by linking two *meso*-positions with acetylene bridges, which allows π-electronic conjugation among the constitutional porphyrins.[32–34] Synthesis of **22** was performed by one-step Glaser–Hay coupling reaction of 5,10-diaryl-15,20-diethynyl nickel porphyrin **23** at 1.0×10^{-3} M in 22% yield (Scheme 7). Separation of **22** was successfully achieved using preparative gel permeation chromatography (GPC). This synthetic procedure was also applied to the larger porphyrin square **24** having 12 porphyrin units. Porphyrin trimer **27** was prepared from the Sonogashira coupling reaction of **25** and **26** under strictly controlled conditions using $AsPh_3$ and $Pd_2(dba)_3{\cdot}CHCl_3$ followed by demetallation, Ni(II) insertion, and *meso*-ethynylation. Tetramerization of **27** *via* Glaser–Hay coupling provided **24** in 9% yield (Scheme 7). Low solubility is often a very serious problem for such large shape-persistent flat molecules, but the porphyrin squares **22** and **24** exhibit reasonably good solubility probably due to Ni(II) metallation.

Smith *et al.* reported the synthesis of cyclic porphyrinoid tetramer **28**.[35] Oxyporphyrin has a hydroxyl substituent at the *meso* position and its keto form exists in the keto–enol

 This journal is © The Royal Society of Chemistry 2007

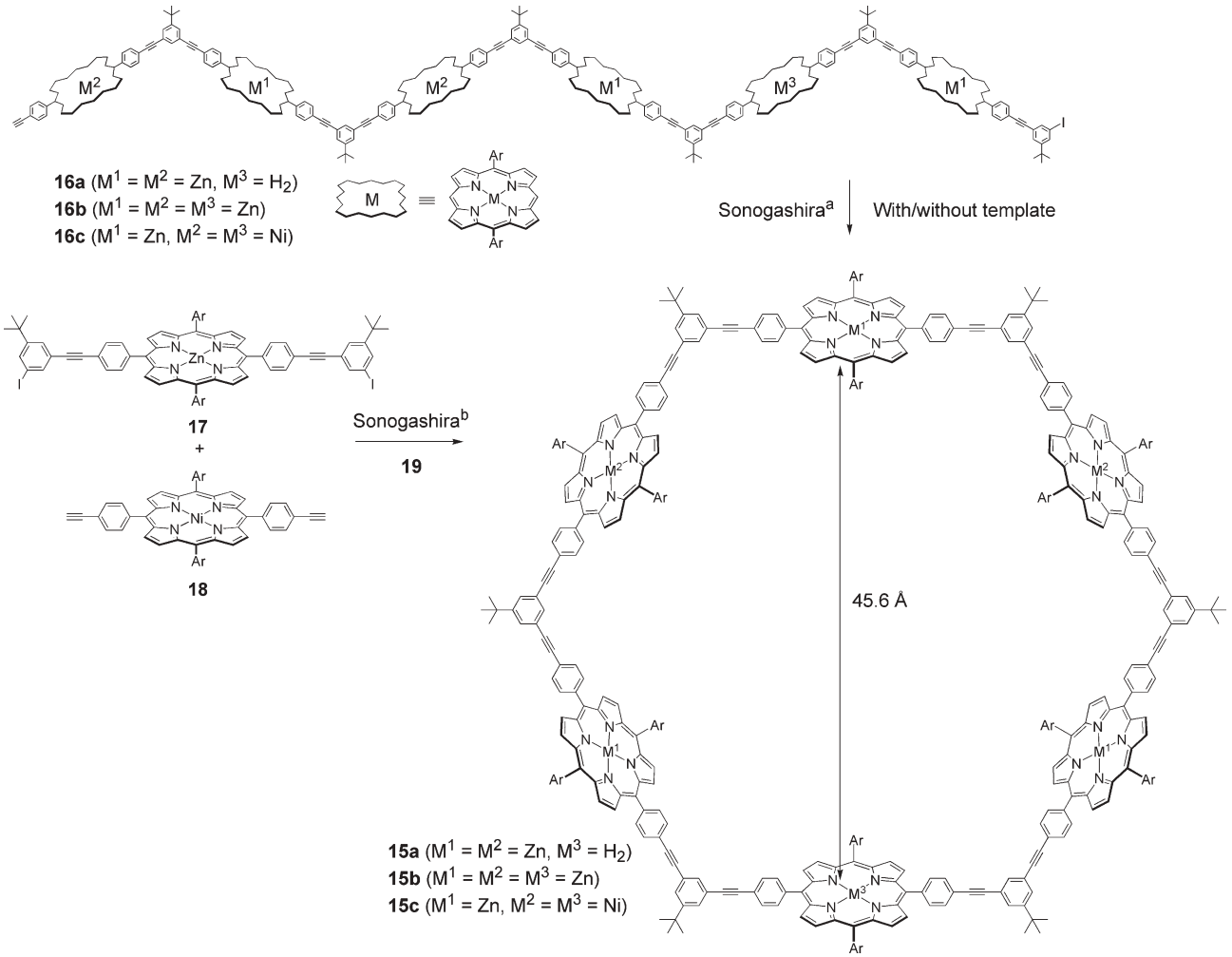

Scheme 5 Reaction conditions: (a) $Pd(PPh_3)_4$, DMF, triethylamine; (b) $Pd_2(dba)_3$, $P(o\text{-tol})_3$, toluene, triethylamine (Ar = mesityl).

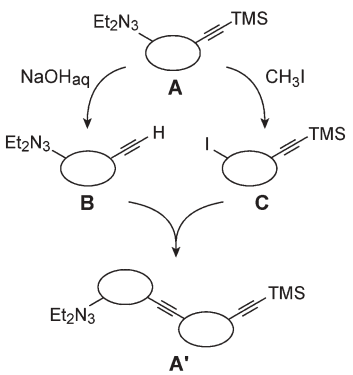

Scheme 6 Iterative coupling sequence.

equilibrium.[36] A remarkable reactivity of oxyporphyrin is its facile oxidative dimerization at the *meso*-positions, which occurs at the 15-position, opposite to the hydroxy-substituted *meso*-position.[37,38] They prepared cyclic tetramer **28** in 93% yield by dimerization of the 1,4-phenylene linked oxyporphyrin dimer **29** upon photo-irradiation in the presence of air (Scheme 8). Interestingly, this dual bond formation reaction is reversible.

Osuka *et al.* reported a variety of porphyrin arrays using a Ag(I)-salt promoted coupling reaction.[39] When a zinc porphyrin possessing unsubstituted *meso* positions is treated with a Ag(I) salt, *meso–meso* linked diporphyrins and oligomeric porphyrins are formed. This coupling reaction is highly regioselective, occurring only at the *meso*-position. A Zn(II) porphyrin monomer substrate is favorable for the coupling reaction owing to its low oxidation potential. Highly regioselective coupling is ascribed to the large electron density at the *meso*-positions in the HOMO of a zinc porphyrin radical cation. To obtain oligomers with the desired number of porphyrins, the reaction conditions should be carefully controlled, including concentration, equivalents of Ag(I) salt, temperature, and reaction time. The remarkable advantages of this coupling reaction are (1) its easy repeatability owing to practically the same coupling reactivities of longer *meso–meso* linked porphyrin arrays and (2) high solubility of long porphyrin arrays. Coupling products were separated through preparative GPC-HPLC by taking advantage of the large difference in the retention time. The longest *meso–meso* linked porphyrin array thus synthesized is a 1024-mer, which is an extremely long monodisperse molecule with a molecular length of *ca.* 0.84 μm.

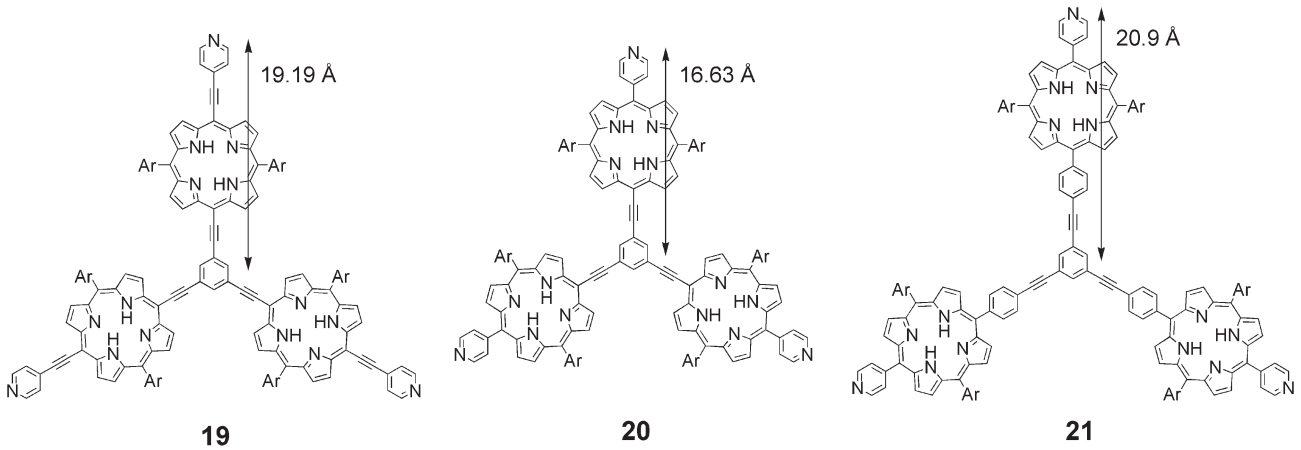

Fig. 2 Structures of templates **19**–**21** (Ar = 3,5-di-*tert*-butylphenyl).

Directly linked cyclic porphyrin arrays **30**, **31** and **32** were synthesized from 5,10-diaryl zinc porphyrin **33** as a starting monomer.[40] By Ag(I)-salt oxidation, dimer **34** and trimers **35a** and **35b** were obtained from **33**, and tetramers **36a** and **36b** were obtained from **34**. In these oligomers, free rotation around the *meso–meso* linkage is strictly prohibited because of

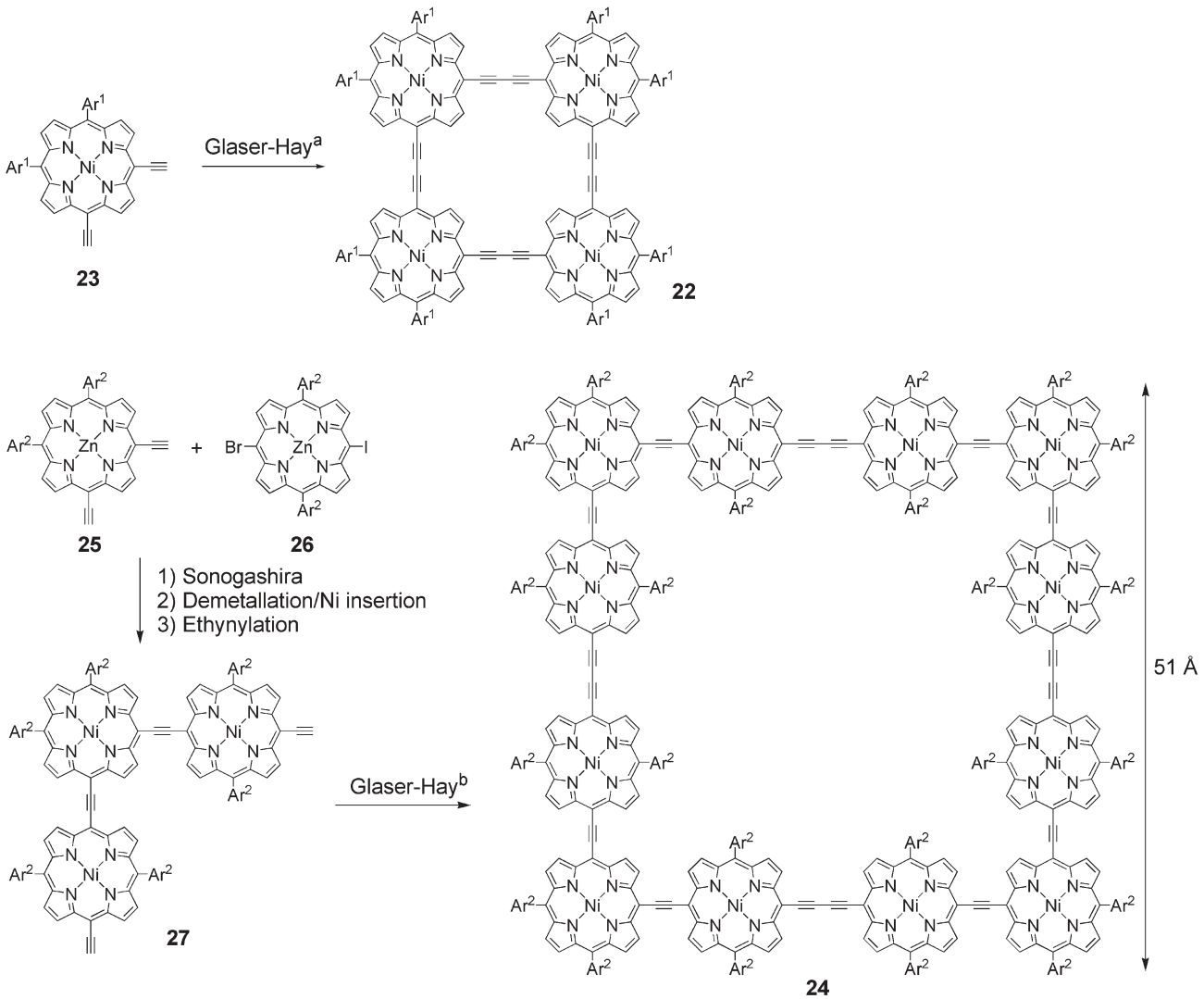

Scheme 7 Reaction conditions: (a) Cu_2Cl_2, TMEDA, CH_2Cl_2; (b) CuCl, TMEDA, CH_2Cl_2, air (Ar^1 = 3,5-di-*tert*-butylphenyl, Ar^2 = 3,5-diisopentylphenyl).

 This journal is © The Royal Society of Chemistry 2007

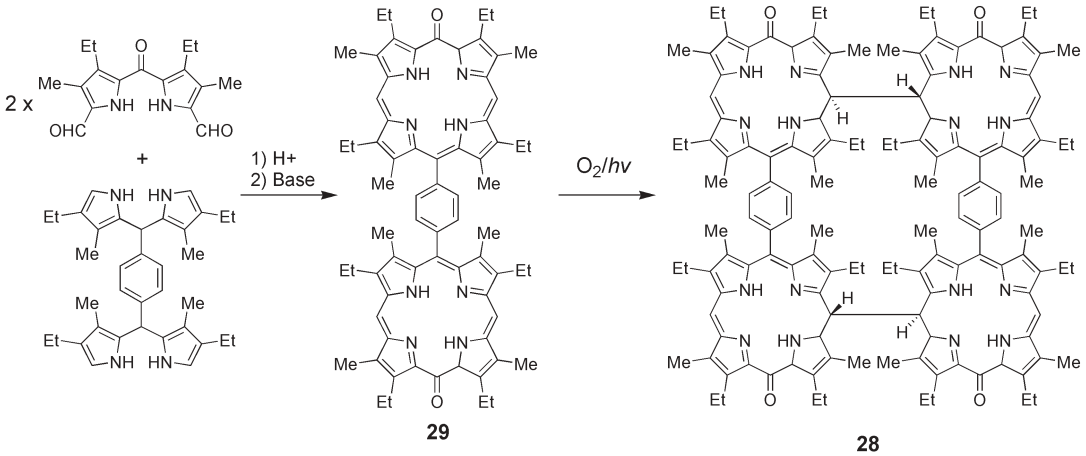

Scheme 8

severe steric hindrance. Among them, **35a** and **36a** which have unsubstituted *meso*-positions on the same side are suitable precursors for cyclic arrays. Cyclic tetramer **30** was synthesized in 74% yield by the intramolecular coupling reaction of **36a** at 2.0×10^{-5} M, whereas the major product changed to cyclic octamer **32** (29%) at 3.3×10^{-3} M (Scheme 9). Cyclic hexamer **31** was synthesized in 22% yield from the coupling reaction of **35a** at 1.0×10^{-4} M (Scheme 9). These cyclic arrays were

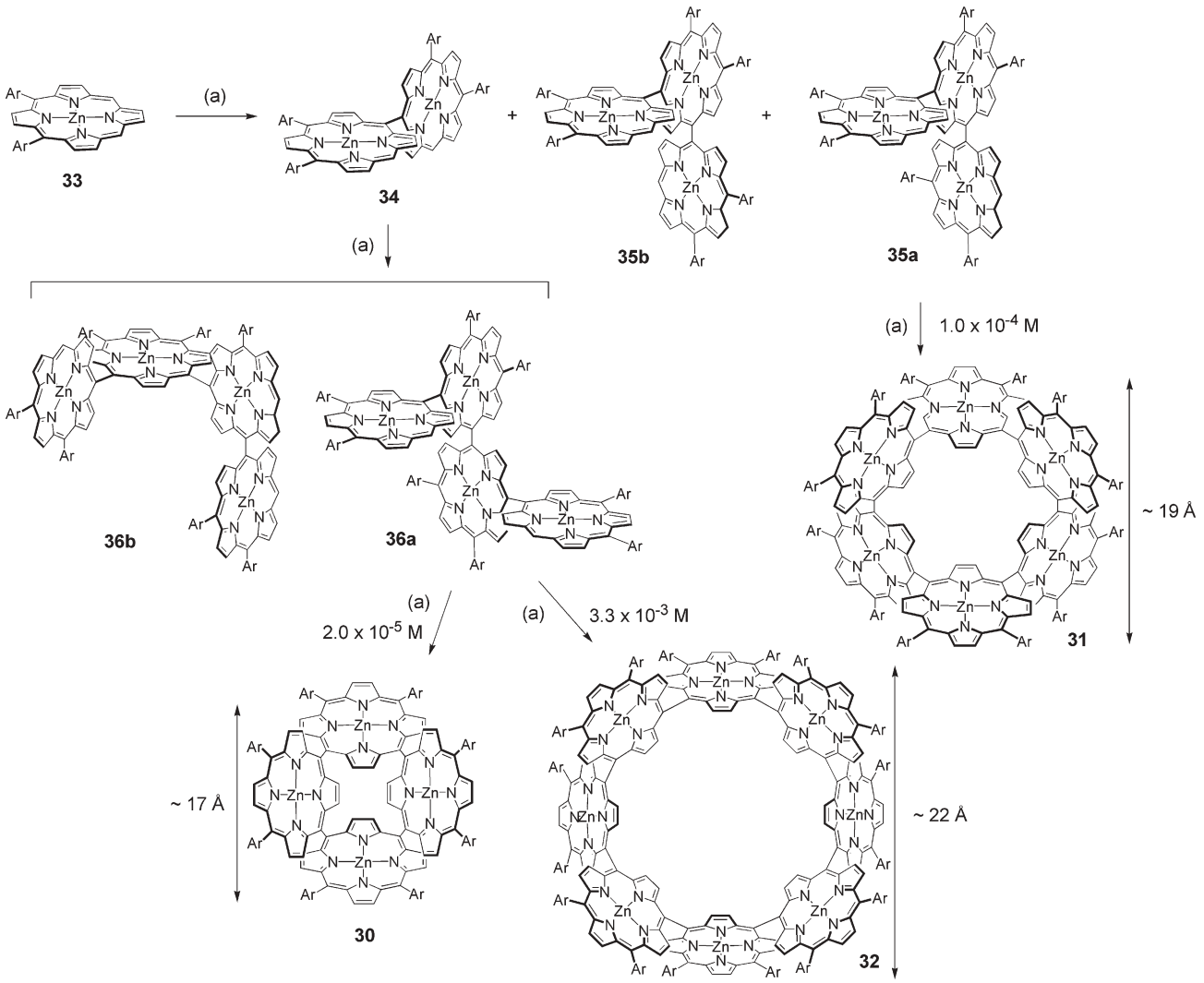

Scheme 9 Reaction conditions: (a) $AgPF_6$, $CHCl_3$ (Ar = 3,5-di-*tert*-butylphenyl).

separated by silica-gel column chromatography, and their structures were fully consistent with their ^{1}H NMR spectra, which are characteristically simple without signals due to *meso*-protons, reflecting the symmetric cyclic structures.

Wheel-like porphyrin oligomers were also synthesized from 1,3-phenylene-bridged *meso–meso* linked porphyrin oligomers.[41,42] Dimer **37** and tetramer **40** were prepared by Suzuki coupling reaction of a *meso*-boronated zinc porphyrin and a *meso*-boronated zinc diporphyrin with 1,3-diiodobenzene, respectively. Repetitive oxidation reactions starting from bridged porphyrin dimer **37** gave linear 12-mer **38**. Using the same reaction procedure, linear precursor 24-mer **41** was obtained from bridged porphyrin tetramer **40**. These acyclic porphyrin arrays were then cyclized by intramolecular coupling under highly diluted conditions (1.0×10^{-6} M) (Schemes 10 and 11). Cyclic compounds were isolated by preparative recycling GPC-HPLC. The isolated yields were 60% for **39** and 34% for **42**. The cyclic structure of **39** was confirmed by its ^{1}H NMR spectrum which lacked signals due to the *meso*-proton, but the ^{1}H NMR spectrum of **42** was rather broad, probably due to structural heterogeneity of such a large molecule.

Use of non-covalent supramolecular interactions has been shown to be beneficial, particularly towards construction of cyclic porphyrin arrays owing to the intrinsic dynamic nature and entropic gain associated with the formation of distinct molecular assemblies rather than polymeric assemblies. Some pioneering work was reported by Hunter *et al.*,[43] and recently Kobuke *et al.* reported the formation of cyclic porphyrin assemblies **45**, **46**, **48**, **49** and **51** from 5-imidazolyl substituted porphyrin dimers **44**, **47**, and **50**, which are bridged by 1,3-phenylene, 1,3-diethynylphenylene, and 5,15-(bis(1,3-phenyl) porphynylene) spacers, respectively (Fig. 3 and 4).[44,45] *meso*-Imidazolyl zinc porphyrin forms the highly stable complementary slipped cofacial dimer **52** with a large association constant of $>10^{10}$ M^{-1}.[46] Zinc insertion in free base dimers resulted in the formation of a polymeric assembly, and subsequent re-organization gave hexameric and pentameric, or trimeric assemblies as main products. Hexameric assembly **45** is considered more energetically favorable than **46** because of the 120° angle of the 1,3-phenylene bridge. Remarkably, Kobuke *et al.* have performed olefin metathesis at the *meso*-substituents, which provided robust assemblies **45C**, **46C**, **48C**, **49C** and **51C**. The parent ion peaks were detected at the expected positions in the mass spectra.

3 Excitation energy transfer along the cyclic arrays

The electronic interactions of neighboring porphyrin chromophores in the arrays are the most important parameters for EET. Such interactions can be evaluated from their absorption spectra. The formation of cyclic porphyrin arrays sometimes induces distortion of the porphyrin ring, which gives rise to a spectral change. More importantly, when incorporated into a cyclic array, the electronic interactions between neighboring porphyrins are changed, reflecting their geometry and different conformational freedom. The simple point-dipole exciton coupling theory developed by Kasha[47] is useful to interpret the spectral changes caused by the inter-chromophore interactions, where the strength of the dipole interaction is represented by Coulombic interactions that depend on the oscillator strength, orientation, and distance. Interaction of the transition dipole moments in a head-to-tail arrangement results in an allowed lower energy transition (J-type coupling), while that in a parallel arrangement results in an allowed higher energy transition (H-type coupling). The spectral changes due to the exciton coupling are most obvious for the Soret bands, since the magnitude of the exciton coupling is

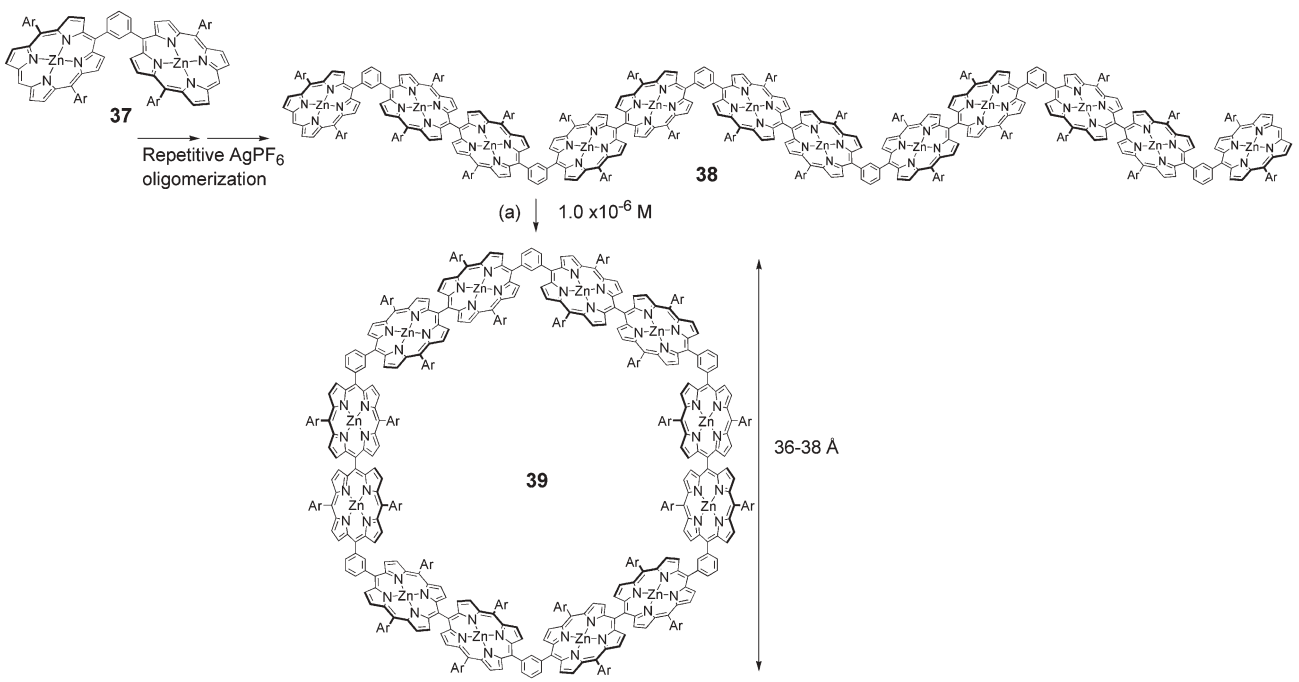

Scheme 10 Reaction conditions: (a) $AgPF_6$, $CHCl_3$ (Ar = *p*-dodecyloxyphenyl).

 This journal is © The Royal Society of Chemistry 2007

proportional to the square of oscillator strength. The components of the Soret band, B_x and B_y, which are degenerate in a porphyrin monomer, independently interact with the transition dipole moments of neighboring porphyrins. Excitonically coupled states are generated in electrostatically interacting porphyrins in a close arrangement. Cyclic porphyrin arrays **8**, **11** and **15** exhibit absorption spectra of the superposition of each porphyrin component, which indicates weak excitonic interaction between them due to long inter-porphyrin distances.

EET processes are the most important function of antenna complexes. Thus, many artificial model compounds have been explored, which absorb visible light in a wide range and funnel the resulting excited-state energy rapidly and efficiently to a designed site. There are two mechanisms for EET, Förster-type (through-space, TS) EET by Coulombic interaction between transition dipole moments and Dexter-type (through-bond, TB) EET *via* electron-exchange interaction through direct or indirect overlap of the wavefunctions.[48,49] The rate of Förster-type EET (k_F) between the energy donor and acceptor is given by eqn (1) and (2):

$$k_F = \frac{9000 \ln 10 \kappa^2 \Phi_f}{128 \pi^5 n^4 \tau_D N_A r^6} J_F \quad (1)$$

$$J_F = \frac{\int F(v)\varepsilon(v)v^{-4}\mathrm{d}v}{\int F(v)\mathrm{d}v} \quad (2)$$

where n is the refractive index of the solvent, N_A Avogadro's number, r the center-to-center distance between two transition dipole moments, κ^2 the orientation factor, Φ_f the fluorescence quantum yield of the donor, τ_D the fluorescence lifetime of the donor, v the wavenumber, and J_F the Förster overlap integral of the luminescence spectrum of the donor ($F(v)$) and the absorption spectrum of acceptor (ε (v)). The rate constant of EET *via* Dexter mechanism (k_D) is formulated as eqn (3)–(5):

$$k_D = \frac{4\pi^2 H^2}{h} J_D \quad (3)$$

$$J_D = \frac{\int F(v)\varepsilon(v)\mathrm{d}v}{\int F(v)\mathrm{d}v \int \varepsilon(v)\mathrm{d}v} \quad (4)$$

$$H = H_0 \exp\left[-\beta(r - r_0)\right] \quad (5)$$

where J_D is the Dexter integral, and β the attenuation factor.

The importance of the orbital interaction on the TB-EET rate was clearly shown by comparison of tetraphenylporphyrin (TPP)-type diporphyrins *versus* octaethylporphyrin (OEP)-type diporphyrins, both of which have the same center-to-center distances between the two porphyrin units (Scheme 12).[50] Interestingly, EET rates in the TPP-type diporphyrins are distinctly larger than those in their OEP-type counterparts but such EET rate enhancement decreases when the distance between the two porphyrins becomes shorter.[51] This rate

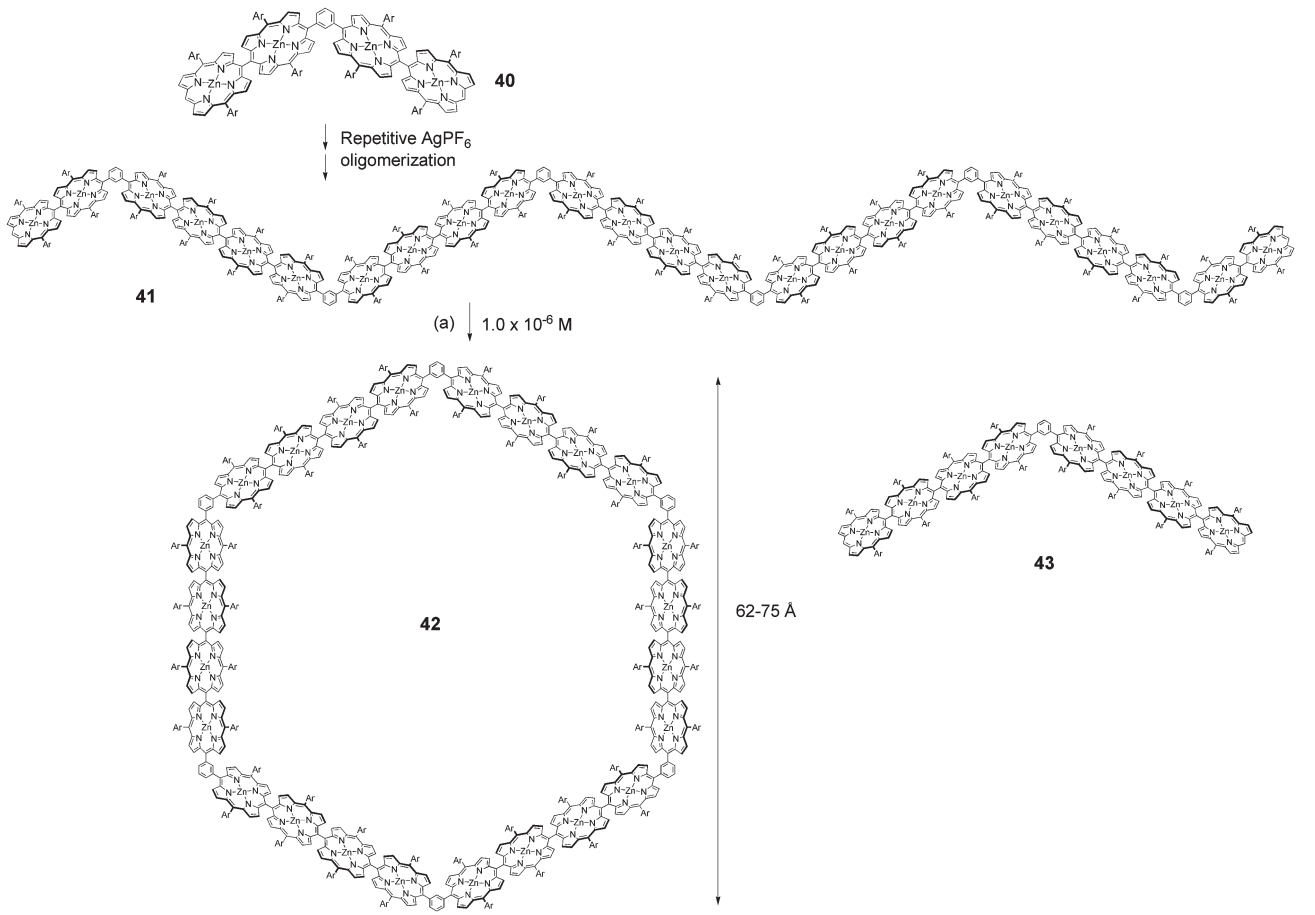

Scheme 11 Reaction conditions: (a) $AgPF_6$, $CHCl_3$ (Ar = *p*-dodecyloxyphenyl).

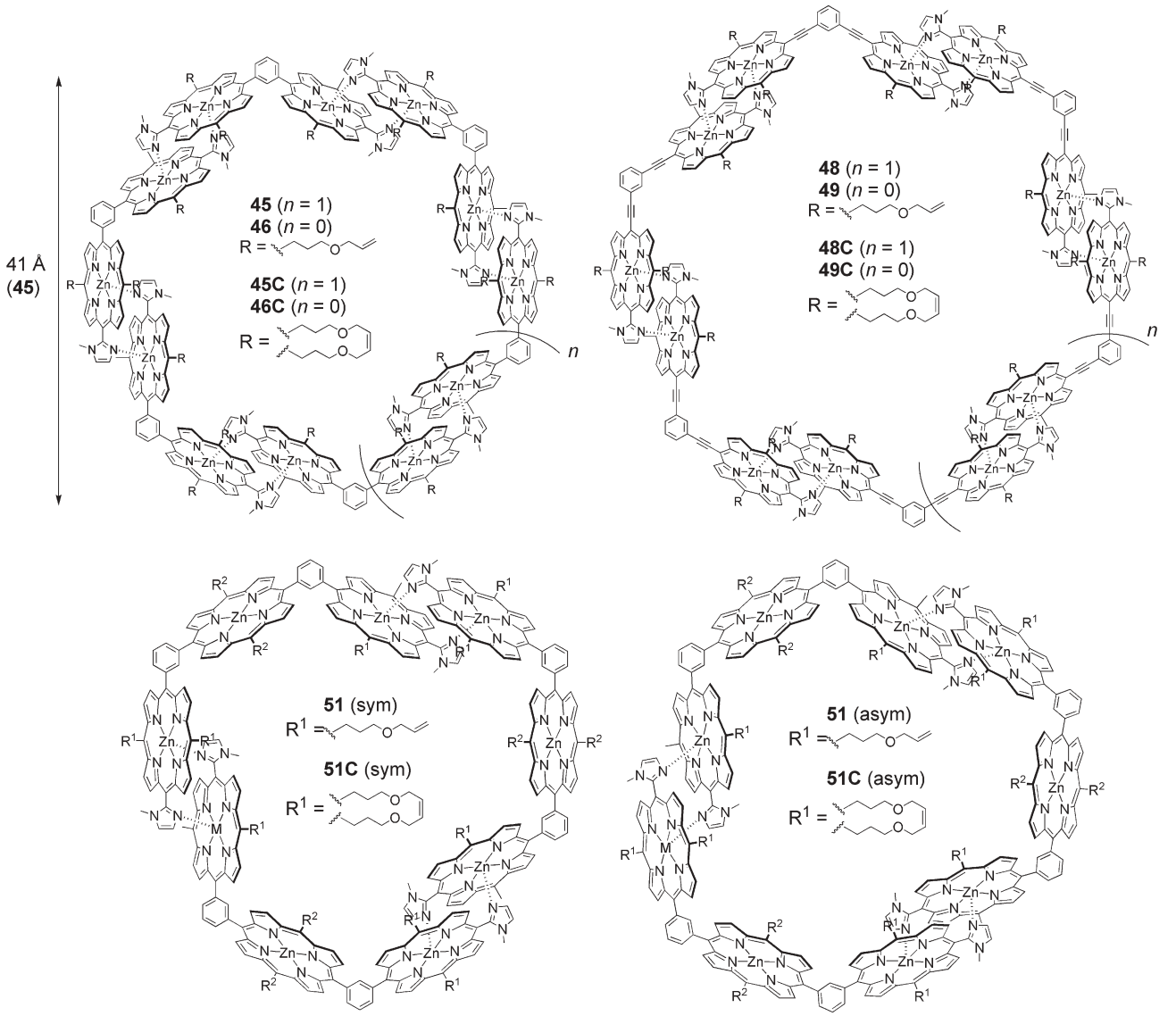

Fig. 3 Structures of Kobuke's cyclic porphyrin assemblies. $R^2 = -(CH_2)_2CO_2CH_3$.

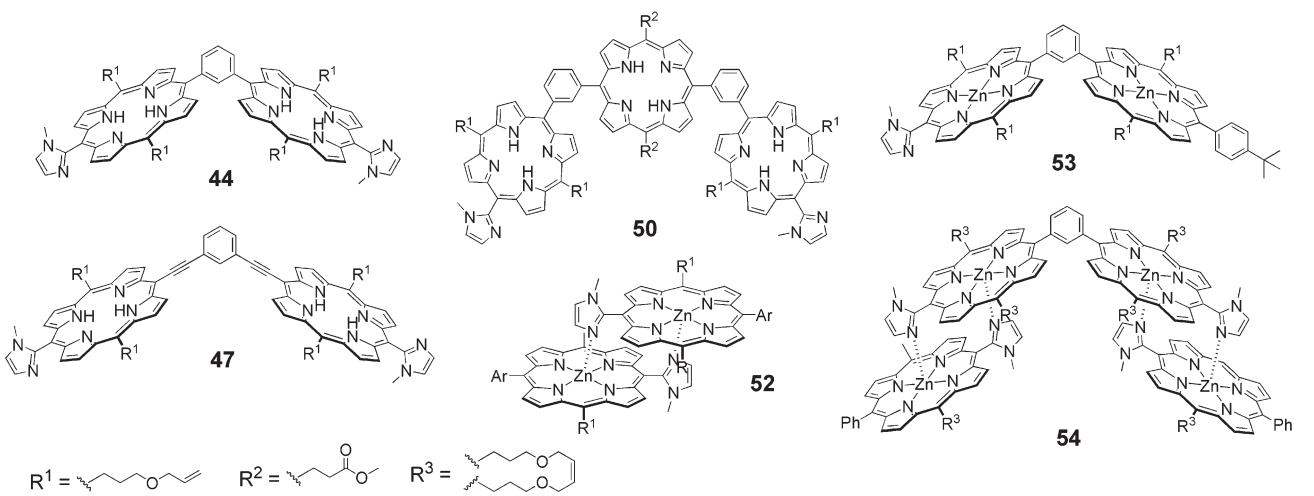

Fig. 4 Structures of Kobuke's precursors.

 This journal is © The Royal Society of Chemistry 2007

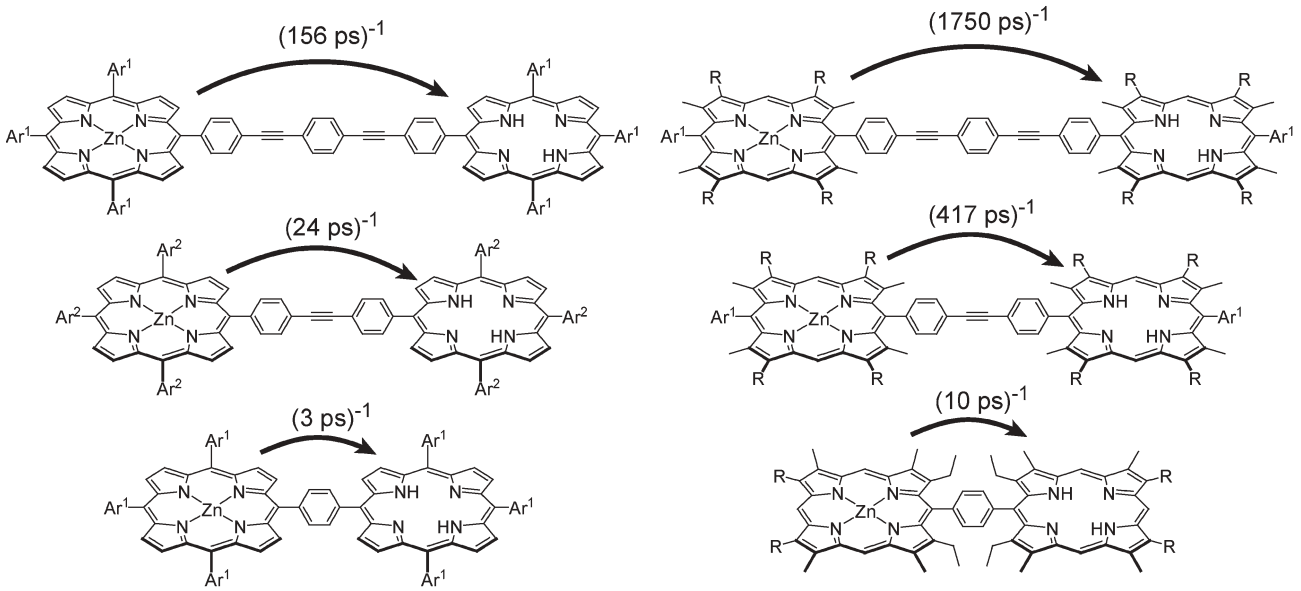

Scheme 12 Excitation energy transfer in diporphyrins (Ar^1 = 3,5-di-*tert*-butylphenyl, Ar^2 = mesityl, and R = C_6H_{13}).

enhancement has been understood in terms of the significant contribution of TB-EET in TPP-type diporphyrin models. It is known that TPP-type zinc porphyrins have an a_{2u} HOMO with large electron densities at the *meso*-positions where unsaturated bridges are connected, while OEP-type zinc porphyrins have an a_{1u} HOMO with nodes at the *meso*-positions (Fig. 5). Therefore, there are effective TB orbital interactions only for TPP-type diporphyrins. In addition, the *meso*-aryl bridges in OEP-type porphyrins are forced to take perpendicular conformations with respect to the porphyrin plane due to steric interactions with the hampering peripheral alkyl substituents, which mitigates the TB electronic interactions. When the bridging group becomes shorter, the EET rate enhancement of TPP-type diporphyrins becomes smaller. This trend can be accounted for in terms of increasing contribution of the Förster mechanism for EET, since Förster EET is steeply accelerated for a donor–acceptor model with quite a short D–A separation.[51] On the contrary, the Förster EET rate decreases quickly with increasing distance between two porphyrin units. The relatively small attenuation of TB-EET *versus* distance for diporphyrins with π-electronic bridges makes TB-EET predominant for diporphyrins with long distances between the porphyrins. As such, the two sets of TPP-type and OEP-type diporphyrins bridged by the same conjugative spacers provide a nice opportunity to demonstrate and evaluate the important contribution of TB-EET in the overall EET processes.

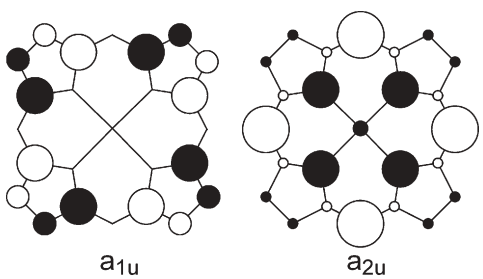

Fig. 5 Schematic representation of the HOMO of the D_{4h} porphyrin.

In B850 in the LH2 antenna of *Rps. acidophila*, the rate of excitation energy hopping rate was estimated to be $(270\ fs)^{-1}$, and the mechanism of this ultrafast energy hopping is considered mainly as a Förster mechanism on the basis of large dipole interactions between cofacial BChl *a*.[52] On the other hand, an interchromophore EET rate constant in B800 of *Rhodobacter sphaeroides* was revealed to be rather small, $(0.8–1.6\ ps)^{-1}$,[53] which was ascribed to a longer distance between neighboring BChl *a* molecules.

The absorption spectra of **8** and **11** are simple superpositions of the spectra of each component, indicating that the dipole interactions in these arrays are negligible and thus the contribution of TS-EET should be small in the whole EET process. The EET rate in **8** from a zinc porphyrin to a free base porphyrin has been determined to be $(26\ ps)^{-1}$. This rate is almost identical to that $(24\ ps)^{-1}$ in **55** bearing the same bridge, which indicated that the rotational restriction of the porphyrin planes in **8** has only a negligible influence on the EET rate because of the small contribution of TS-EET.[29b,c] The EET rate of **11a** is $(34\ ps)^{-1}$, which is similar to that ($(40\ ps)^{-1}$) of **56** but is smaller than that ($(24\ ps)^{-1}$) of the linear dimer **55** (Scheme 13). Slower EET in **56** than that in **55** is explained in terms of unfavorable orbital interaction through a 3,4′-diphenylethynyl spacer, as compared to that through a 4,4′-diphenylethynyl spacer.

Characteristically, *meso–meso* linked porphyrin arrays exhibit split Soret bands due to exciton coupling. The Soret band of a Zn(II) porphyrin originates from two perpendicular components B_x and B_y. In a simple monomer, they are degenerate, but in a *meso–meso* linked diporphyrin they couple differently. B_x transition dipole moments along the *meso–meso* bond are excitonically coupled to generate an allowed lower energy transition (B_x + $B_{x'}$), while the mutual coulombic

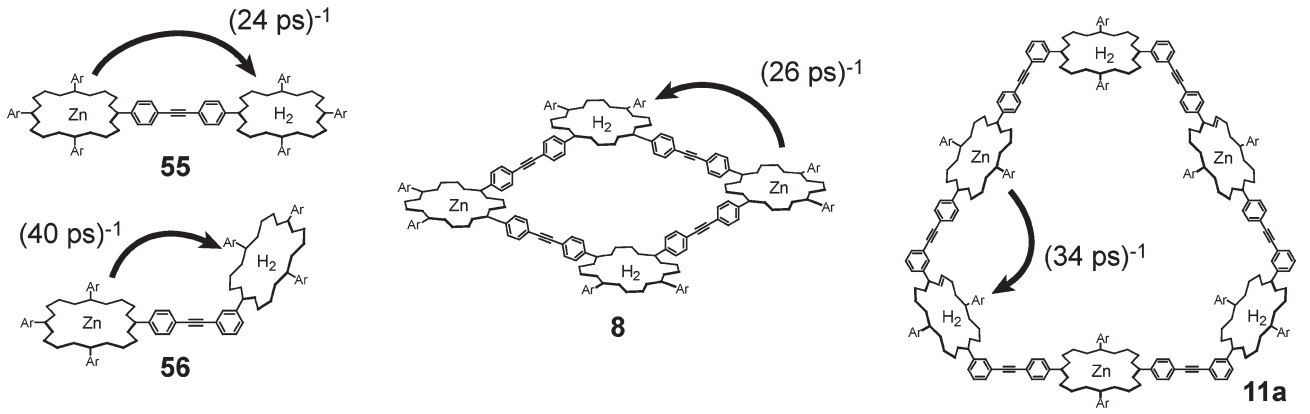

Scheme 13 Excitation energy transfer within porphyrin arrays.

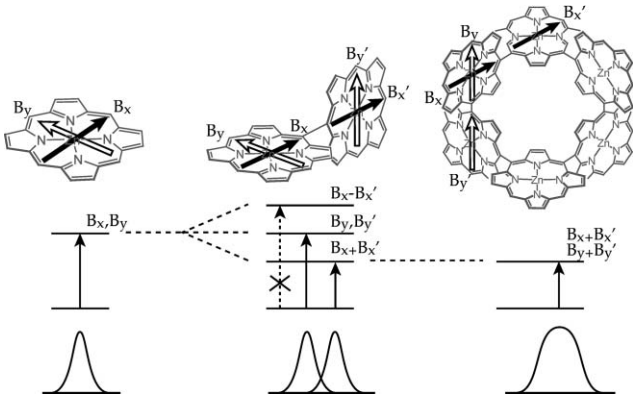

Fig. 6 Exciton coupling models of *meso–meso* linked porphyrin oligomers.

interactions of B_y transition dipole moments are canceled due to their orthogonal conformation. Consequently, the Soret band of *meso–meso* linked linear porphyrin arrays is split into a red-shifted band and an unperturbed band (Fig. 6).

In contrast to these linear *meso–meso* linked porphyrin arrays, directly *meso–meso* linked cyclic porphyrin arrays exhibit a broad red-shifted Soret band (Fig. 6). In the cyclic arrays, both the transition dipole moments B_x and B_y are excitonically coupled with those of the neighboring porphyrins to cause an excitonically allowed state of the same energy. As described above, the linear *meso–meso* linked porphyrin arrays exhibit J-type exciton coupling along the long molecular axis, but H-type coupling is also possible when the array is bent as seen for **30** and **32**, in which the dihedral angles of neighboring porphyrin rings deviate from 90°. The dihedral angles of neighboring porphyrin planes are calculated to be *ca.* 72°, 90°, and 77° for **30**, **31**, and **32**, respectively, which are well consistent with the ^{1}H NMR results. The Soret band of tetramer **30** has a small peak at the higher energy side, which has been assigned to H-type coupling, considering the non-negligible components of neighboring dipole moments having an almost parallel-like orientation.

The EET rates in **30**, **31** and **32** were determined by transient absorption (TA) and transient absorption anisotropy (TAA) measurements. In TA measurements, pump-power dependent decay causes the singlet–singlet excitation annihilation process due to Förster-type incoherent EET within the array.[52,54,55] EET processes in the directly linked cyclic arrays are quite efficient with rate constants of $(119\ \text{fs})^{-1}$ for **30**, $(342\ \text{fs})^{-1}$ for **31**, and $(236\ \text{fs})^{-1}$ for **32**, which rival those in B850 of the natural cyclic antenna system (Scheme 14). These efficient EET arise from extremely strong excitonic coupling between

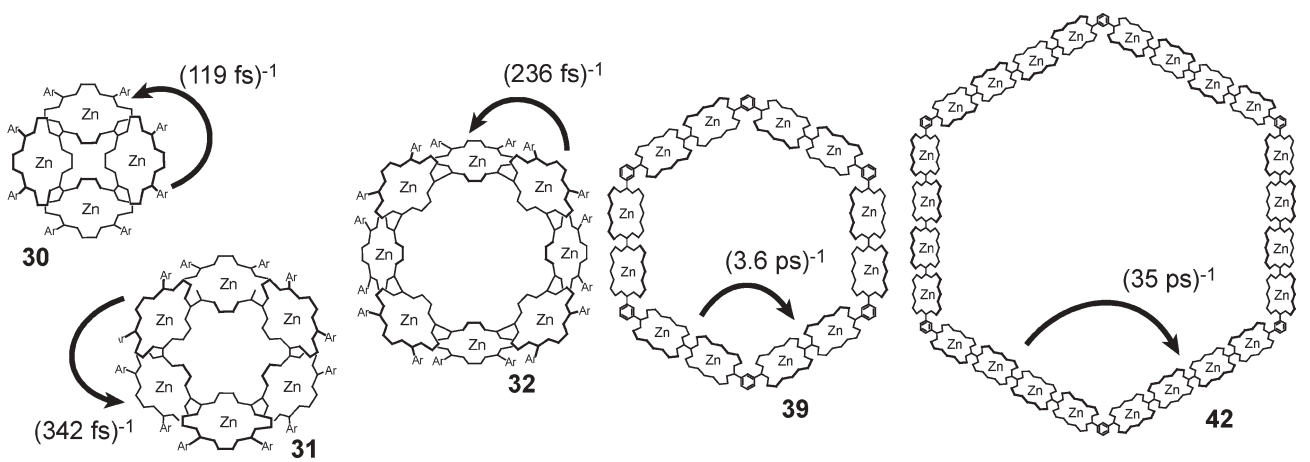

Scheme 14 Excitation energy transfer within porphyrin arrays.

 This journal is © The Royal Society of Chemistry 2007

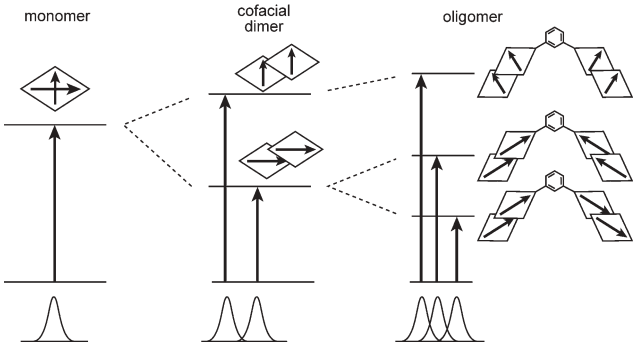

Fig. 7 Exciton coupling models of imidazole-substituted porphyrin oligomers.

porphyrin components. The observed order of EET rates of **31** < **32** < **30** is the same as the order of electronic communication between neighboring porphyrin units, as estimated from their absorption spectra and calculated dihedral angles between neighboring porphyrins.

The absorption spectra of **39** and **42** are quite similar to those of dimer **40** and tetramer **43** components respectively. These data indicate that the electronic interactions are dominated by exciton coupling within *meso–meso* linked porphyrin subunits. Significant differences in the absorption spectra between acyclic arrays and cyclic arrays are shoulder peaks in the spectra of **38** and **41**, which correspond to the terminal monomer or dimer moiety, respectively, and are not observed in the spectra of the cyclic arrays **39** and **42**.

The EET rates in **39** and **42** have been determined similarly by TA and TAA to be $(3.6\ \text{ps})^{-1}$ and $(35\ \text{ps})^{-1}$, respectively (Scheme 14). These rates are almost the same as those of the respective references, **40** and **43**. In these arrays, the excited state is considered to be delocalized over the dimeric or tetrameric porphyrin subunit.[56] Based on these data, the EET processes in **39** and **42** have been interpreted by means of a Förster-type EET model. A large difference between the EET rates of **39** and **42** is explained in terms of a large difference in the center-to-center distance of *meso–meso* linked porphyrin subunits. This distance in **42** is *ca*. 1.5-fold longer than that in **39**, which, on the basis of the distance factor of R^{-6} in the Förster EET equation, explains well the observed about 10-fold difference in the EET rate.

The absorption spectrum of slipped-cofacial imidazole porphyrin dimer **52** exhibits a largely split Soret band, indicating strong exciton coupling between closely positioned two porphyrin rings (Fig. 7). Compared to the split Soret band of **45C**, cyclic array **48C** exhibits a broad Soret band similar to those of other 1,3-bis-ethynylphenyl bridged porphyrin arrays. This is due to long-range exciton coupling between cofacial diporphyrins, since a 1,3-bis-ethynylphenyl bridge can take a planar conformation with regard to the connected porphyrins.

In the cyclic porphyrin arrays developed by Kobuke *et al.*, the excitation energy is well delocalized in a mutually imidazole-coordinating cofacial diporphyrin subunit. EET rates of **45C** and **46C** were determined to be $(5.3\ \text{ps})^{-1}$ and $(8.0\ \text{ps})^{-1}$, respectively, which are faster than those of the reference compounds, $(9.4\ \text{ps})^{-1}$ for **53** and $(9.2\ \text{ps})^{-1}$ for **54**. These results may indicate the importance of rigid conformations of the cyclic arrays that are favorable for efficient EET.[57] Although electronic communication between the two bridged porphyrins is stronger in **48C** and **49C** than in phenylene bridged assemblies, their EET rate constants over the bridge are smaller, $(12.8\ \text{ps})^{-1}$ and $(21\ \text{ps})^{-1}$, as compared to **45C** and **46C** respectively (Scheme 15), which can be accounted for in terms of the longer distances of coherent cofacial dimers. In both the phenylene and diethynylphenyl bridged assemblies, the hexameric assemblies exhibited the faster EET.

Table 1 summarizes the data of the EET of the cyclic porphyrin arrays. In every case, efficient EET has been observed, which allows many circulations of excitation energy hopping along the array, considering the rather long lifetimes of the excited singlet of a zinc porphyrin (1.5–2 ns). The EET rate is primarily determined by the center-to-center distance of neighboring porphyrins. Very efficient EET processes with rates of <1 ps that rival those in the natural LH2 have been only achieved for directly *meso–meso* linked cyclic porphyrin arrays **30**, **31**, and **32**, in which very close spatial arrangements lead to extremely large Förster-type interactions.

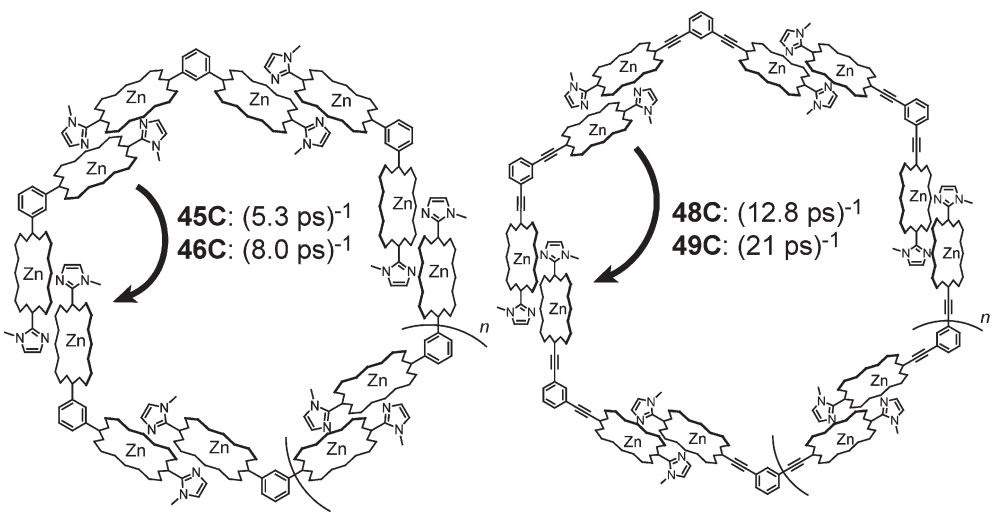

Scheme 15 Excitation energy transfer within porphyrin assemblies.

Table 1 Data of EET in cyclic porphyrin arrays

Compound	Number of porphyrin	r/Å[a]	Mechanism[b]	Rate constant[c]
8	4	20[c]	D	$(26\ \text{ps})^{-1}$
11a	6	17.6	D	$(34\ \text{ps})^{-1}$
30	4	5.3–5.9	F	$(0.12\ \text{ps})^{-1}$
31	6	6.0	F	$(0.34\ \text{ps})^{-1}$
32	8	6.0–6.1	F	$(0.24\ \text{ps})^{-1}$
39	12	17–19	F	$(3.6\ \text{ps})^{-1}$
42	24	31–33	F	$(35\ \text{ps})^{-1}$
45C	12	16[c]	F	$(5.3\ \text{ps})^{-1}$
46C	10	16[c]	F	$(8.0\ \text{ps})^{-1}$
48C	12	20[c]	F	$(12.8\ \text{ps})^{-1}$
49C	10	20[c]	F	$(21\ \text{ps})^{-1}$

[a] Center-to-center distance. [b] Predominant mechanism of EET, Förster (F), Dexter (D). [c] Roughly estimated in our hands.

4 Complexation of cyclic porphyrin arrays with guest molecules

Inspired by the structure of the core antenna–reaction center complex, guest inclusion by a cyclic porphyrin array has been attempted. Quite high affinities of cyclic porphyrin host molecules **4** and **15c** towards porphyrin-based guest molecules have been reported.[27,28,58] The association constant of **4** with tetrapyridyl porphyrin **7** is $2 \times 10^{10}\ \text{M}^{-1}$, which indicates the formation of the complex even at micromolar concentrations of host and guest molecules. The binding ability of **15c** was examined for guest molecules of variable size, and the association constants determined are listed in Table 2. Interestingly, **20**, which showed a poor templating ability for the synthesis of **15c**, exhibited the largest association constant.

Lindsey *et al.* reported the formation of the 1 : 1 complex of **11b** with bipodal molecule **57** (Fig. 8).[59] While the fluorescence spectrum of guest-free host **11b** is identical to that of the zinc porphyrin monomer component, that of the **11b**·**57** complex taken by excitation at 550 nm (Zn(II) porphyrin Q-band) displays a large contribution from the emission from the free base porphyrin guest, indicating EET from the cyclic zinc porphyrin host to the guest. EET efficiency from the coordinated zinc porphyrin to the guest free base porphyrin was determined to be 40%, which is nearly the same as the value (44%) estimated on the basis of the Förster mechanism. The TB-EET process between **11b** and **57** in this complex is inefficient reflecting insufficient electronic communication of the pyridyl moiety with the porphyrin ring at the zinc atom.

The zinc atoms not used for the construction of cyclic array of **51** can serve as coordination sites for guest molecules. Tetrapodal guest molecule **58** was successfully incorporated into the cavity of **51** with an association constant of $8 \times 10^8\ \text{M}^{-1}$ (Fig. 9). This type of tetrapodal guest molecule possesses an extra arm not used for the complexation, which can be fabricated for EET study.

Table 2 Association constants (K) between **15c** and guest molecules

Guest	K/M^{-1}
19	2.8×10^9
20	3.4×10^9
21	1.8×10^9

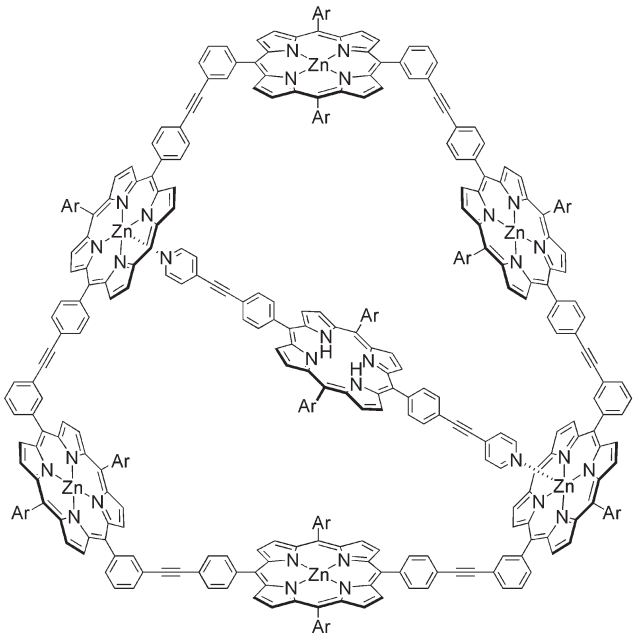

Fig. 8 Molecular structure of the complex **11b**·**57**.

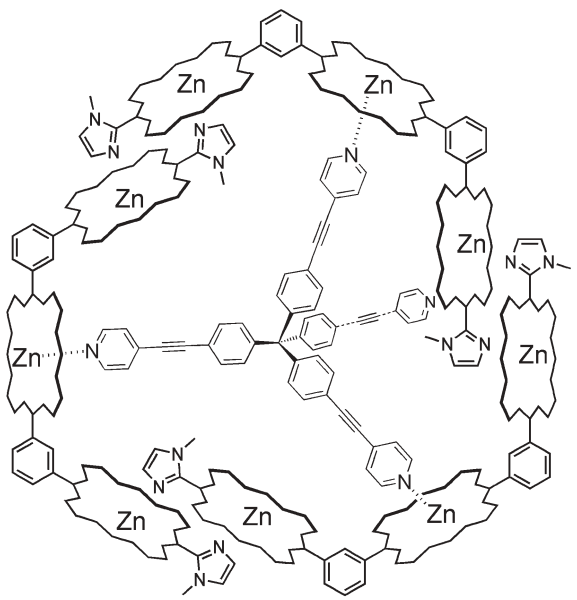

Fig. 9 Molecular structure of the complex **51**·**58**.

5 Conclusions

Recent progress in the exploration of covalently linked cyclic porphyrin arrays as artificial photosynthetic antennae has been reviewed with particular attention to synthetic methods and excitation energy transfer (EET). The final difficult cyclization steps have been often accomplished with the aid of templates. Efficient EET along the wheel is observed in these cyclic arrays, but ultrafast EET with rates $>(1\ \text{ps})^{-1}$ that rival those in the natural LH2 is rare and has been only identified for cyclic arrays **30–32** composed of directly *meso–meso* linked porphyrins. Hence, these studies help reveal the structural requirements for efficient EET. In addition, these

This journal is © The Royal Society of Chemistry 2007

shape-persistent arrays are promising structural units for even larger functional aggregates. Therefore, cyclic porphyrin arrays of novel structures will remain an attractive synthetic target in the future.

References

1 G. McDermott, S. M. Prince, A. A. Freer, A. M. Hawthornthwaite-Lowless, M. Z. Papiz, R. J. Cogdell and N. W. Isaacs, *Nature*, 1995, **374**, 517.
2 J. Koepke, X. Hu, C. Muenke, K. Schulten and H. Michel, *Structure*, 1996, **4**, 581.
3 A. W. Roszak, T. D. Howard, J. Southall, A. T. Gardiner, C. J. Law, N. W. Isaacs and R. J. Cogdell, *Science*, 2003, **302**, 1969.
4 M. R. Wasielewski, *J. Org. Chem.*, 2006, **71**, 5051.
5 D. Gust, T. A. Moore and A. L. Moore, *Acc. Chem. Res.*, 2001, **34**, 40.
6 H. Imahori and Y. Sakata, *Adv. Mater.*, 1997, **9**, 537.
7 H. Imahori, *Org. Biomol. Chem.*, 2004, **2**, 1425.
8 W. M. Campbell, A. K. Burrell, D. L. Officer and K. W. Jolley, *Coord. Chem. Rev.*, 2004, **248**, 1363.
9 K. Sugiura, *Top Curr. Chem.*, 2003, **228**, 65.
10 A. K. Burrell, D. L. Officer, P. G. Pleiger and D. C. W. Reid, *Chem. Rev.*, 2001, **101**, 2751.
11 J. K. M. Sanders, in *Porphyrin Handbook*, ed. K. M. Kadish, K. M. Smith and R. Guilard, Academic Press, New York, 2000, vol. 3, p. 347.
12 T. Imamura and K. Fukushima, *Coord. Chem. Rev.*, 2000, **198**, 133.
13 J. Wojaczyński and L. Latos-Grażyński, *Coord. Chem. Rev.*, 2000, **204**, 113.
14 E. Iengo, E. Zangrando and E. Alessio, *Eur. J. Inorg. Chem.*, 2003, 2371.
15 F. Würthner, C.-C. You and C. R. Saha-Möller, *Chem. Soc. Rev.*, 2004, **33**, 133.
16 A. Satake and Y. Kobuke, *Tetrahedron*, 2005, **61**, 13.
17 H. L. Anderson and J. K. M. Sanders, *J. Chem. Soc., Chem. Commun.*, 1989, 1714.
18 H. L. Anderson and J. K. M. Sanders, *Angew. Chem., Int. Ed. Engl.*, 1990, **29**, 1400.
19 S. Anderson, H. L. Anderson and J. K. M. Sanders, *Angew. Chem., Int. Ed. Engl.*, 1992, **31**, 907.
20 L. G. Mackay, R. S. Wylie and J. K. M. Sanders, *J. Am. Chem. Soc.*, 1994, **116**, 3142.
21 R. W. Wagner, J. Seth, S. I. Yang, D. Kim, D. F. Bocian, D. Holten and J. S. Lindsey, *J. Org. Chem.*, 1998, **63**, 5042.
22 J. Li, A. Ambroise, S. I. Yang, J. R. Diers, J. Seth, C. R. Wack, D. F. Bocian, D. Holten and J. S. Lindsey, *J. Am. Chem. Soc.*, 1999, **121**, 8927.
23 L. Yu and J. S. Lindsey, *J. Org. Chem.*, 2001, **66**, 7402.
24 D. Holten, D. F. Bocian and J. S. Lindsey, *Acc. Chem. Res.*, 2002, **35**, 57.
25 R. W. Wagner, T. E. Johnson, F. Li and J. S. Lindsey, *J. Org. Chem.*, 1995, **60**, 5266.
26 O. Mongin, A. Schuwey, M.-A. Vallot and A. Gossauer, *Tetrahedron Lett.*, 1999, **40**, 8347.
27 S. Rucareanu, O. Mongin, A. Schuwey, N. Hoyler and A. Gossauer, *J. Org. Chem.*, 2001, **66**, 4973.
28 S. Rucareanu, A. Schuwey and A. Gossauer, *J. Am. Chem. Soc.*, 2006, **128**, 3396.
29 J. Zhang, D. J. Pesak, J. L. Ludwick and J. S. Moore, *J. Am. Chem. Soc.*, 1994, **116**, 4227.
30 J. S. Moore, *Acc. Chem. Res.*, 1997, **30**, 402.
31 J. S. Schumm, D. L. Pearson and J. M. Tour, *Angew. Chem., Int. Ed. Engl.*, 1994, **33**, 1360.
32 K. Sugiura, Y. Fujimoto and Y. Sakata, *Chem. Commun.*, 2000, 1105.
33 A. Kato, K. Sugiura, H. Miyasaka, H. Tanaka, T. Kawai, M. Sugimoto and M. Yamashita, *Chem. Lett.*, 2004, **33**, 578.
34 H. L. Anderson, *Chem. Commun.*, 1999, 2323.
35 R. G. Khoury, L. Jaquinod, D. J. Nurco, R. K. Pandey, M. O. Senge and K. M. Smith, *Angew. Chem., Int. Ed. Engl.*, 1996, **35**, 2496.
36 A. H. Jackson, G. W. Kenner and K. M. Smith, *J. Chem. Soc. C*, 1968, 302.
37 J.-H. Fuhrhop, E. Baumgartner and H. Bauer, *J. Am. Chem. Soc.*, 1981, **103**, 5854.
38 A. L. Balch, B. C. Noll, S. L. Philips, S. M. Reid and E. P. Zovinka, *Inorg. Chem.*, 1993, **32**, 4730.
39 N. Aratani, A. Takagi, Y. Yanagawa, T. Matsumoto, T. Kawai, Z. S. Yoon, D. Kim and A. Osuka, *Chem.–Eur. J.*, 2005, **11**, 3389.
40 Y. Nakamura, I.-W. Hwang, N. Aratani, T. K. Ahn, D. M. Ko, A. Takagi, T. Kawai, T. Matsumoto, D. Kim and A. Osuka, *J. Am. Chem. Soc.*, 2005, **127**, 236.
41 X. Peng, N. Aratani, A. Takagi, T. Matsumoto, T. Kawai, I.-W. Hwang, T. K. Ahn, D. Kim and A. Osuka, *J. Am. Chem. Soc.*, 2004, **126**, 4468.
42 T. Hori, N. Aratani, A. Takagi, T. Matsumoto, T. Kawai, M.-C. Yoon, Z. S. Yoon, S. Cho, D. Kim and A. Osuka, *Chem.–Eur. J.*, 2006, **12**, 1319.
43 X. Chi, A. J. Guerin, R. A. Haycock, C. A. Hunter and L. D. Sarson, *J. Chem. Soc., Chem. Commun.*, 1995, 2563.
44 Y. Kuramochi, A. Satake and Y. Kobuke, *J. Am. Chem. Soc.*, 2004, **126**, 8668.
45 F. Hajjaj, Z. S. Yoon, M.-C. Yoon, J. Park, A. Satake, D. Kim and Y. Kobuke, *J. Am. Chem. Soc.*, 2006, **128**, 4612.
46 Y. Kobuke and H. Miyaji, *J. Am. Chem. Soc.*, 1994, **116**, 4111.
47 M. Kasha, H. R. Rawls and M. A. El-Bayoumi, *Pure Appl. Chem.*, 1965, **11**, 371.
48 (*a*) T. Förster, *Ann. Phys.*, 1948, **2**, 55; (*b*) T. Förster, *Discuss. Faraday Soc.*, 1959, **27**, 7.
49 D. L. Dexter, *J. Chem. Phys.*, 1953, **21**, 836.
50 D. Holten, D. F. Bocian and J. S. Lindsey, *Acc. Chem. Res.*, 2002, **35**, 57.
51 H. S. Cho, D. H. Jeong, M.-C. Yoon, Y. H. Kim, Y.-R. Kim, D. Kim, S. C. Jeoung, S. K. Kim, N. Aratani, H. Shinmori and A. Osuka, *J. Phys.Chem. A*, 2001, **105**, 4200.
52 G. Trinkunas, J. L. Herek, T. Polivka, V. Sundström and T. Pullerits, *Phys. Rev. Lett.*, 2001, **86**, 4167.
53 S. Hess, F. Feldchtein, A. Babin, I. Nurgaleev, T. Pullerits, A. Sergeev and V. Sundström, *Chem. Phys. Lett.*, 1993, **216**, 247.
54 S. E. Bradforth, R. Jimenez, F. van Mourik, R. van Grondelle and G. R. Fleming, *J. Phys. Chem.*, 1995, **99**, 16179.
55 B. Brüggemann, J. L. Herek, V. Sundström, T. Pullerits and V. May, *J. Phys. Chem. B*, 2001, **105**, 11391.
56 N. Aratani, H. S. Cho, T. K. Ahn, S. Cho, D. Kim, H. Sumi and A. Osuka, *J. Am. Chem. Soc.*, 2003, **125**, 9668.
57 I.-W. Hwang, M. Park, T. K. Ahn, Z. S. Yoon, D. M. Ko, D. Kim, F. Ito, Y. Ishibashi, S. R. Khan, Y. Nagasawa, H. Miyasaka, C. Ikeda, R. Takahashi, K. Ogawa, A. Satake and Y. Kobuke, *Chem.–Eur. J.*, 2005, **11**, 3753.
58 S. Anderson, H. L. Anderson, A. Bashall, M. McPartlin and J. K. M. Sanders, *Angew. Chem., Int. Ed. Engl.*, 1995, **34**, 1096.
59 A. Ambroise, J. Li, L. Yu and J. S. Lindsey, *Org. Lett.*, 2000, **2**, 2563.